The nonconventional design obtained after the rotation of the parent ellipsoid may present an XPOL degradation due to the fact that the minimum XPOL conditions—Mizugutch and Rusch conditions [9], [10]—are no longer satisfied. Our solution to this problem is to alter the value of the subreflector eccentricity, while keeping all orientation angles constant. In general, eccentricity values greater than the one employed before the rotation will reduce system XPOL. The synthesis algorithm implemented in DORA produces a low cross-polarized (-35-dB or better) dual-offset Gregorian antenna which has adequate clearance between the feed axis and the bottom of the main reflector. In addition, the resulting configuration has the ability to operate with either an LP or a circularly polarized (CP) feed over a wide bandwidth without the need of being repositioned (no substantial beam squint). The GBT radio telescope is to be illuminated by CP feeds and, therefore, beam squint must be carefully taken into account for proper operation. Detailed information on CP feeds and beam squint can be found in [8].

V. Conclusions

The electrical performance of the GBT reflector antenna was evaluated with the commercial code GRASP7 and the code PRAC. The code DORA, developed by the authors, was employed to upgrade the GBT single-offset configuration to a low cross-polarized dual-offset Gregorian reflector configuration. The results from DORA are in very good agreement with published ones [1]. The procedure implemented in DORA, as discussed in this paper, uses the main reflector as a fixed input parameter, a feature that makes DORA especially recommended for the GBT case example, given that the GBT offset main reflector once built cannot be easily changed. New designs for the GBT suboptics assembly can be obtained with DORA if the subreflector size, or other parameter such as the feed configuration, is changed.

The computer simulations confirmed a low XPOL level when the GBT dual configuration is illuminated by a purely polarized feed antenna. A single feed antenna or array with high XPOL will likely degrade the total system XPOL performance. Finally, a procedure was described to reduce XPOL in dual-offset Gregorian reflector antennas while attending practical manufacturing constraints, such as an adequate feed region clearance. An effort was made to present the main conclusions as generically as possible.

References

[1] S. Srikanth, "Comparison of spillover loss of offset Gregorian and Cassegrain antennas," in *IEEE AP-S Symp. Dig.*, London, U.K./Canada, June 1991, pp. 444–447.
[2] R. Hall and L. J. King, "The Green Bank Telescope," in *IEEE AP-S Symp. Dig.*, Chicago, IL, July 1992, pp. 862–865.
[3] M. A. B. Terada and W. L. Stutzman, "Computer-aided design of reflector antennas," *Microwave J.*, pp. 64–73, Aug. 1995.
[4] M. A. B. Terada and W. L. Stutzman, "Design of offset–parabolic-reflector antennas for low cross-pol and low sidelobes," *IEEE Antennas Propagat. Mag.*, vol. 35, pp. 46–49, Dec. 1993.
[5] Y. Rahmat-Samii and V. Galindo-Israel, "Shaped reflector antenna analysis using the Jacobi–Bessel series," *IEEE Trans. Antennas Propagat.*, vol. AP-28, pp. 425–435, July 1980.
[6] C. Scott, *Modern Methods of Reflector Antenna Design.* Norwood, MA: Artech House, 1990.
[7] W. L. Stutzman and G. A. Thiele, *Antenna Theory and Design*, 2nd ed. New York: Wiley, 1997.
[8] M. A. B. Terada and W. L. Stutzman, "Cross polarization and beam squint in single and dual offset reflector antennas," *Electromagnetics J.*, vol. 16, no. 6, pp. 633–650, Nov./Dec. 1996.
[9] Y. Mizugutch, M. Akagawa, and H. Yokoi, "Offset dual reflector antenna," in *IEEE AP-S Symp. Dig.*, Amherst, MA, Oct. 1976, pp. 2–5.
[10] K. W. Brown, Y. H. Lee, and A. Prata, Jr., "A systematic design procedure for classical offset dual reflector antennas with optimal electrical performance," in *IEEE AP-S Symp. Dig.*, Ann Arbor, MI, July 1993, pp. 772–775.

Recirculating Loop for Experimental Evaluation of EDFA Saturated Regime Effects on Optical Communication Systems

Claudio Mazzali and Hugo L. Fragnito

***Abstract*—We demonstrate an optical-fiber recirculating loop for experimental simulation of long-haul optical communication systems using cascaded erbium-doped fiber amplifiers (EDFA's) operating in the gain saturation regime. The loop contains sections of dispersion shifted fibers (DSF's), standard fiber, and a set of in-line devices, such as tuning filters, optical amplifiers, polarization controllers, and a variable attenuator. The main results presented here are related to the observation of the effects due to the slow dynamics of the EDFA. We also discuss the validity of using an optical attenuator to simulate an extra length of fiber.**

***Index Terms*—Optical amplifiers, optical communications, recirculating loops.**

I. Introduction

Optical recirculating loops are useful tools for experimental simulations of long-distance communications (>100 km) where the performance of system components can be evaluated at a greatly reduced cost as compared to straight transmission experiments or field tests. Fiber loops with erbium-doped fiber amplifiers (EDFA's) can be used to experimentally investigate new transmission concepts such as dispersion management, solitons, and wavelength division multiplexing (WDM), and study, for example, the fundamental limits of ultra-long-distance linear and nonlinear (soliton) communications [1]–[4]. In these studies, the EDFA's operate in the linear gain regime and, thus, simulate a link with EDFA's spaced at 25–50 km. There is considerable recent interest in links with booster amplifiers separated by distances >100 km so as to minimize the number of amplifiers and reduce the system cost.

In this paper, we analyze the behavior of fiber loops when the EDFA's operate in the saturated gain regime. Fig. 1 shows a schematic of our experimental setup. The optical devices and their positions within the loop are changed for different experiments, thus we present in Fig. 1 a standard setup just for the purpose of discussing the main features of fiber loops

The signal source is a mode-locked erbium-doped fiber laser that generates 10-ps pulses at a repetition rate of 2.5 GHz [5]. The output from this laser is amplified by a booster EDFA and switched on and off by a lithium–niobate electro-optic switch that modulates the train

Manuscript received December 10, 1997; revised December 10, 1997. This work was supported by CNPq, Telebrás, Fapesp, Finep, PADCT, and the Brazilian Ministry of Science and Technology under the PRONEX Program.

The authors are with the Instituto de Física Gleb Wataghin-DEQ, UNICAMP, Campinas, CEP 13.083–970, São Paulo, Brazil.

Publisher Item Identifier S 0018-9480(98)02029-8.

0018–9480/98$10.00 © 1998 IEEE

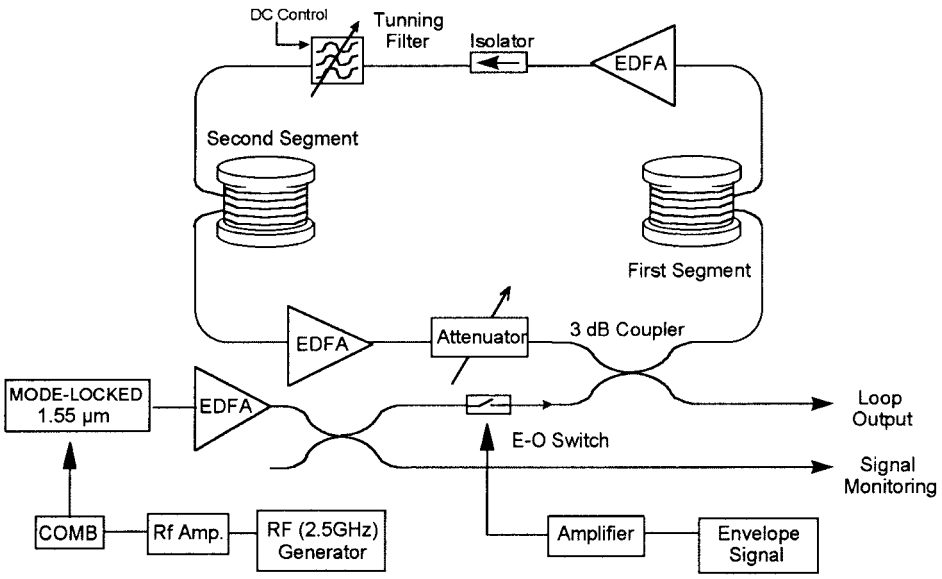

Fig. 1. Experimental loop configuration.

of picosecond pulses in a packet with a duration shorter than the loop round-trip time.

The packet is injected into the loop through a 3-dB coupler which also acts as the output coupler. We have one or two segments of single-mode optical fiber (standard or dispersion shifted, depending on the experiment objective) inside the loop, and two EDFA's operating in gain saturation regime, a tunable (Fabry–Perot) filter to reduce the amount of amplified spontaneous emission (ASE) in the loop, and an optical isolator that is essential to reject the back reflection generated by the Fabry–Perot filter. Since there is another amplifier before the output coupler, the observed recirculating signal is always superimposed to the ASE from this second amplifier, giving a background level that was used to normalize the data in Fig. 2.

There are some parameters that characterize a loop transmission experiment. The fundamental parameters are the number of loop transits N, the total propagated distance $L_{\rm tot} = NL$ (L is the loop length), and the total time of flight of photons in the loop $T_{\rm tot} = NT$ (T is the loop round-trip time).

There is a limit in the number of loop cycles (and, thus, the total distance that the experiment can simulate) given by the growth of ASE noise from the optical amplifiers. If the total loop gain (G) equals or exceeds the loop loss (Γ) at a given wavelength, then the loop will lase at that wavelength. Thus, some mechanism must be provided to delay the buildup of laser action before the signal pulse has completed the N loop cycles. However, in very long-distance experiments, the lasing buildup time can be smaller than $T_{\rm tot}$. A simple way to prevent laser oscillation in loops with Raman or semiconductor amplifiers is through a dynamic control of the amplifier pump [6], [7], but this technique cannot be used with EDFA's due to the slow response of the Erbium ion populations. Buildup of noise and lasing in this case can be prevented by the use of a bandpass spectral filter centered at the signal wavelength or by using a synchronized electro-optic modulator that keeps the loss high, except during the time slots where the signal pulses pass through the modulator [8]. Another technique that can be used for soliton experiments is the sliding guiding-filter technique, where an electronically tunable filter has its bandpass slightly shifted in each loop cycle, thus providing high loss for the linear noise and a relative transparent path for the soliton, which self adjusts its spectrum [9]. Finally, another technique explored in this paper is to saturate the gain of the EDFA's. This technique is discussed in Section II.

II. Effects Due to the Gain Dynamics of EDFA

The first result that we present here is the propagation of a packet of pulses over 33 turns in a loop formed by two EDFA's and 45 km of fiber (25 km of dispersion shifted fiber (DSF) for the first segment and 20 km of standard fiber for the second segment). This experiment simulates the propagation over 1485 km in a straight line with optical amplifiers separated by 20 and 25 km.

The electro-optic switch in Fig. 1 modulates the continuous train of pulses at 2.5 Gb/s with a flat-top envelope of 140-μs width, which corresponds to keep 62% of the 45-km loop filled with optical pulses (T for 45 km is 225 μs). The envelope repetition rate is 130 Hz to allow for the observation of several loop turns before the injection of the next packet. The signal at the loop output is shown in Fig. 2. In this experiment, we see 33 packets (33 turns) between two consecutive injections.

The first packet in Fig. 2 is a replica of the injected one, and each subsequent packet corresponds to an increasing number of transits in the fiber loop. Note that the injected packet has an optical power smaller than that observed after the first turn; this means the total loop gain is larger than the total loop loss. As discussed above, under this condition the loop eventually becomes a ring laser oscillator. However, the first packet has enough energy to significantly saturate the gain of the two EDFA's in the loop, thus the second (and each of all subsequent packets) sees a gain which is smaller than the loop loss, as is confirmed by the decreasing amplitude of the subsequent packets. Thus, we demonstrate that it is possible to prevent laser oscillation of the loop by saturating the gain of the EDFA's.

The saturated regime is also confirmed by the decreasing amplitude inside the packet, as can be observed in the inset in Fig. 2 (third packet). If the EDFA's were operating in the linear gain regime, one would observe a decay of the packet amplitude over consecutive round trips, but the quasi-exponential decay inside the packet can only be due to the saturated amplifiers.

These results display a time evolution which is related to the dynamics of the saturated loop gain. For the purpose of clarifying the discussion, we have drawn in Fig. 2 two dashed lines, one

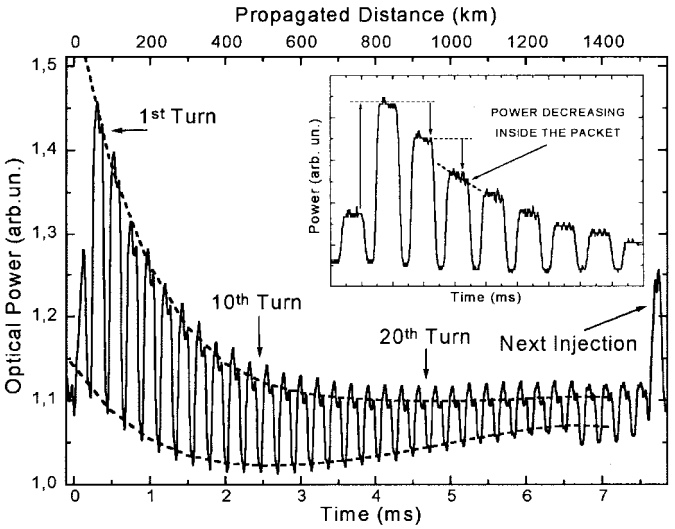

Fig. 2. Transmission through the 45-km loop over 33 turns (1485 km). Intensity normalized by the background ASE level.

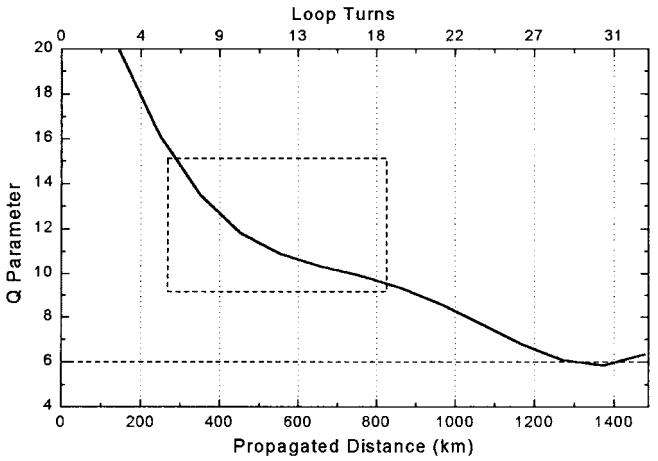

Fig. 3. Q-parameter as a function of the propagation distance (bottom axis) and loop turns (top axis).

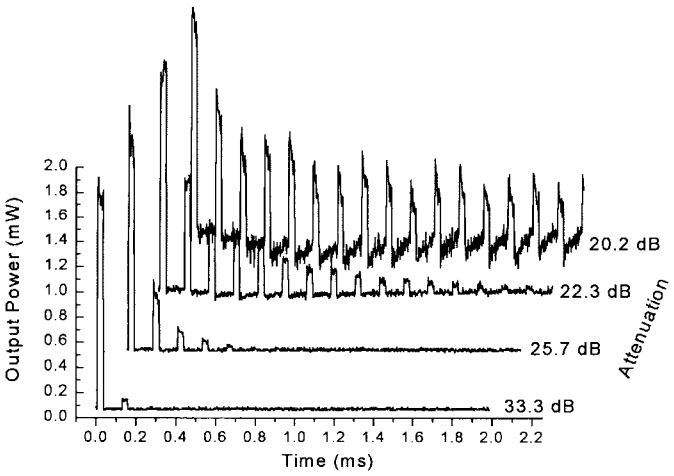

Fig. 4. Signal evolution after successive transits though the recirculating loop for different settings of the variable attenuator in Fig. 1.

passing through the packet amplitudes and another passing through the baselines between adjacent packets. The baseline also displays a nonlinear behavior. These two curves (dashed lines) reflect the population dynamics of an EDFA and are usually disregarded because this dynamics is so slow when compared to the bit period in telecommunications systems. However, as this experiment shows, the slow gain dynamics of the EDFA's should be considered when the transmission is in the form of packets with interleave times that permits a nonsteady-state operation of the amplifiers.

When a modulated signal propagates in the presence of ASE noise in a saturated amplifier, part of the signal modulation is transferred to the noise. The baseline shown in Fig. 2 is a measure of the nonmodulated noise and displays a minimum near the tenth turn (500 km). After this point, the gain starts to recover. Note that the baseline grows faster than the amplitude line, indicating that the nonmodulated noise grows at a larger rate than the modulated signal. Near the thirtieth turn (1300 km), it is apparent that the noise is also modulated. A useful way of describing noisy signals is through the Q-parameter, defined as the (optical power) signal-to-noise ratio (SNR), where noise is the sum of noises of levels "0" and "1." The result is presented in Fig. 3. For the distance range ($<$1200 km) where the modulated noise is negligible small, the Q-parameter decreases monotonically with distance, as expected. Also note that for all loop turns in this range, the Q-parameter is larger than six (horizontal dashed line). This indicates that the bit error rate (BER) is smaller than 10^{-9}, which is a standard value for reliable optical communications systems [10], [11]. The shoulder shown in Fig. 3 (between 300–800 km) is most likely due to the recovery of the gain.

III. Recirculating Fiber Loop With Variable Length of Fiber

In this section, we experimentally simulate a link with periodic booster EDFA's operating in the gain saturation regime and with a large separation distance between amplifiers. The loop configuration is similar to that shown in Fig. 1, but with only one segment of 25 km of DSF. We use a variable optical attenuator (as well as other elements with fixed insertion loss, as described below) to simulate a variable extra length of fiber in the range of 70 km (minimum total loop loss $\Gamma = 14$ dB) to 250 km (maximum $\Gamma = 50$ dB). In this manner, we simulate a system with identical amplifiers separated by the same distance $L_{\rm eq}$. By varying $L_{\rm eq}$, we can investigate, for example, the minimum number of amplifiers in order to reach a total transmission distance $NL_{\rm eq}$ for a given SNR. We analyze the balance between gain and loss to keep the SNR larger than a given acceptable value.

The linear gain of the EDFA was set at 26 dB. The total insertion loss from the 25 km of fiber, optical isolator, 3-dB coupler, spectral filter, splices, and fiber connectors was 15 dB, corresponding to the loss of 75 km of fiber (assuming fibers with 0.2-dB/km loss). We used a variable attenuator to simulate the loss that would be introduced by an extra span of fiber whose length could be varied in the range of 20 km ($-$4-dB minimum insertion loss) to 200 km ($-$40 dB). Thus, for example, with 35 dB in the variable attenuator, the total loop loss is $\Gamma = 50$ dB, corresponding to an effective length of $L_{\rm eq} = 250$ km of fiber. In this example, the loop would simulate a link with booster amplifiers separated by $L_{\rm eq} = 250$ km. Fig. 4 shows the measured output signal after successive transits trough the loop. Each sequence of pulses in this figure was obtained for different values of insertion loss, Γ_a in the variable attenuator, and each 30-μs pulse is an envelope of a train of 10-ps pulses at a rate of 2.5 GHz. The second observable envelope pulse has propagated one cycle trough the loop ($N = 1$), the third corresponds to $N = 2$, and so on. The time between two adjacent envelopes $T = 125$ μs coincides with the expected value for the loop period assuming 25 km of fiber (with a refractive index of 1.5).

For $\Gamma_a = 33.3$ dB (total loop loss $\Gamma = 43.9$ dB, effective loop length $L_{\rm eq} = 241.5$ km), the attenuation is so large that only the first loop round trip can be observed. For $\Gamma_a = 20.2$ dB (total loop loss $\Gamma = 35.2$ dB, effective loop length $L_{\rm eq} = 176$ km), we observed the propagation for 16 turns in the loop, which results in 400 km of actual fiber or 2816 km of equivalent fiber. For $\Gamma_a < 20.2$ dB, the ASE level is too large and eventually the loop becomes a laser.

As N increases, the optical SNR degrades and a limit exists for the number of loop cycles that keeps the SNR above a given value. We have used the same argument of the previous section that relates the BER to the Q-parameter to determine a propagation distance limit where useful communication can take place with an acceptable reliability. For example, with $\Gamma_a = 23.7$ dB (total loop loss $\Gamma = 34.3$ dB, effective loop length $L_{\rm eq} = 171.5$ km), the condition $Q > 6$ limits the number of loops cycles to $N = 6$ (total effective span of $NL_{\rm eq} = 1029$ km). For the case of $\Gamma_a = 20.2$ dB, the limit was $N = 16$.

In this type of loop experiment, we claim that transmission through 25 km of fiber followed by an optical attenuator of, say, 35 dB is equivalent to a transmission experiment through $L_{\rm eq} = 200$ km of fiber. Furthermore, we claim that, say, 16 turns in such a loop is equivalent to a transmission experiment through $NL_{\rm eq} = 3200$ km with amplifiers separated by 200 km. These assertions need to be qualified and commented. There are two main concerns here since the effects of dispersion and nonlinearity accumulated in 1250 km of fiber are not the same as those accumulated in the actual 250 km of fiber. Let us comment on dispersion first. The dispersion parameter D of our DSF fiber is $D = 0.1$ ps/nm/km at 1.55 μm, and assuming a laser linewidth of $\delta\lambda = 0.2$ nm, the group delay dispersion is below 0.02 ps/km. At 2.5 Gb/s, we can assume a time slot for each bit of 200 ps for return to zero (RZ). Thus, a single 10-ps bit broadens its pulse duration to 200 ps only after 4000 km in the broad spectrum case and 15 000 km in the bandwidth limited case (our laser pulses are bandwidth limited and have hyperbolic secant squared shape). Clearly, the dispersion introduced by 3200 km of DFS would be not enough to reduce the transmission performance at 2.5 Gb/s.

The second point is nonlinearity. This is governed by the effective length where nonlinear optical effects in fibers occur: $L_{\rm eff} = (1 - e^{-\alpha L})/\alpha = 20$ km for $\alpha = 0.2$ dB/km and $L \gg \alpha$. Thus, 25 km of DS fiber introduces approximately the same nonlinearities than 200 km of the same fiber. One can argue that once the pulses becomes broadened by self-phase modulation (SPM) in the first 20 km of fiber, the dispersion in the remaining 180 km of a 200-km span may be relevant. To contest this, we can say that spectral broadening is certainly $\Delta\lambda < \delta\lambda$. Using $\Delta = (\lambda n_2 L_{\rm eff}/A_{\rm eff}\, c)\; dP/dt$ [12], where the nonlinear refractive index $n_2 = 2.3 \times 10^{-16}$ cm^2/W, effective area of $A_{\rm eff} = 50$ μm^2 (as is typical of DSF), and a maximum power derivative $dP/dt = 3$ mW/ps, we estimate the expected spectral broadening from SPM in $L_{\rm eff} = 20$ km as $\Delta\lambda = 0.2$ nm. These equations can be used to analyze the validity limits of loop experiments also for other fiber types. For our experiments, nonlinear optical and dispersion effects are not relevant and the propagation through the 25 DSF followed by an attenuation of 35 dB is a good representation of the propagation through 200 km of fiber. Of course, this argument applies to single wavelength transmission, but not to WDM systems. For these cases, interference between channels due to four wave mixing (FWM) must be considered [13], and we should measure the pulses themselves and not just the packet envelopes. Actually, in the case of nonlinearities, the DSF is even worst since it permits a larger interaction length of different channels and, consequently, increase the penalty by FWM.

It should be clear that our experiments were designed specifically to analyze the effects of EDFA dynamics on packet transmission. Our loop technique is very convenient for this purpose because of the slow time response of erbium population which allows a clear visualization of its effects on the packet amplitude.

IV. Conclusions

We presented a recirculating fiber loop for experimental simulations of long-distance optical communication systems using saturated gain EDFA's.

In one experiment, we show that even when the linear gain exceeds the loop loss, buildup of laser action can be inhibited by gain saturation. In this experiment, we demonstrated the propagation over more than 33 turns in a 45-km fiber loop (1400 km). The gain dynamics of the EDFA's considerably affect the SNR, but error-free $(Q > 6)$ transmission is possible for at least 1300 km (and probably more, as we did not attempt to optimize this limit).

In a second experiment, we investigated the possibility of simulating a variable extra length of DSF through the inclusion of a variable attenuator inside the loop. In this case, we propagated trains of 10-ps pulses for an equivalent distance of 2800 km with $Q > 6$. The conditions for the validity of this simulation depend on the dispersion and nonlinear optical effects of the fiber being simulated and the pulse parameters.

Recirculating fiber loops are very useful setups to experimentally study propagation effects in optical communication systems, joining flexibility, reliability, and a low operational cost. Fiber loops can also be very interesting as optical memories to store megabits of data that can be used in fast data buffer applications or even for dispersion compensation schemes.

References

[1] L. F. Mollenauer, M. J. Neubelt, S. G. Evangelides, J. P. Gordon, J. R. Simpson, and L. G. Cohen, "Experimental study of soliton transmission over more than 10 000 km in dispersion shifted fiber," *Opt. Lett.*, vol. 15, no. 21, pp. 1203–1205, 1990.

[2] D. J. Malyon, T. Widdowson, E. G. Bryant, S. F. Carter, J. V. Wright, and W. A. Stalland, "Demonstration of optical pulse propagation over 10 000 km of fiber using recirculating loop," *Electron. Lett.*, vol. 27, no. 2, pp. 120–121, 1991.

[3] N. Bergano, J. Aspell, C. R. Davidson, P. R. Trischitta, B. M. Nyman, and F. W. Kerfoot, "Bit error rate measurements of 14 000 km 5 Gbit/s fiber amplifier transmission system using recirculating loop," *Electron Lett.*, vol. 27, no. 21, pp. 1889–1890, 1991.

[4] M. Nakazawa, E. Yamada, H. Kubota, and K. Suzuki, "10 Gbit/s soliton data transmission over one million kilometers," *Electron. Lett.*, vol. 27, no. 14, pp. 1270–1272, 1991.

[5] C. Mazzali and H. L. Fragnito, "Tunable and high bit rate erbium-doped fiber ring soliton source," in *Opt. Amplifiers Applicat., Tech. Dig.* (Optical Society of America), Washington, DC, 1997, pp. 239–242.

[6] E. Desurvire, M. J. F. Digonnet, and H. J. Shaw, "Raman amplification of recirculating pulses in a reentrant fiber loop," *Opt. Lett.*, vol. 10, no. 2, pp. 83–85, 1985.

[7] ——, "Theory and implementation of a Raman active fiber delay line," *J. Lightwave Technol.*, vol. LT-4, pp. 426–443, Apr. 1986.

[8] M. Nakazawa, H. Kubota, E. Yamada, and K. Suzuki, "Infinite-distance soliton transmission with controls in time and frequency domains," *Electron. Lett.*, vol. 28, no. 12, pp. 1099–1100, 1992.

[9] L. F. Mollenauer, E. Litchman, M. J. Neubelt, and G. T. Harvey, "Demonstration using sliding frequency guiding filters, of error free soliton transmission over more than 20 000 km at 10 Gbit/s, single channel and over more than 13 000 km at 20 Gbit/s in a two-channel WDM," presented at the Opt. Fiber Commun. (OFC/IOOC) Conf., (Optical Society of America), Washington, DC, 1993, paper PD8.

[10] G. P. Agrawal, *Fiber-Optic Communication Systems.* New York: Wiley, 1992.

[11] G. Keiser, *Optical Fiber Communications*, 2nd ed. New York: McGraw-Hill, 1991.

[12] D. Grischowsky and A. C. Balant, "Optical pulse compression based on enhanced frequency chirping," *Appl. Phys. Lett.*, vol. 41, no. 1, pp. 1–3, 1982.

[13] R. W. Tkach, A. R. Chraplyvy, F. Forghieri, A. H. Gnauck, and R. M. Derosier, "Four-photon mixing and high-speed WDM systems," *J. Lightwave Technol.*, vol. 13, pp. 841–849, May 1995.

A Time–Frequency Analysis Method for Radar Scattering

Haralambos N. Kritikos and Joseph G. Teti, Jr.

***Abstract*—A time–frequency analysis method to study electromagnetic scattering is presented and demonstrated using canonical objects. The time–frequency analysis method utilizes the Bargmann transform to formulate the signal representation in phase space. The use of the Bargmann transform leads to an attractive parametric signal representation in terms of complex polynomials, and elliptical filters can be constructed to crop or extract selected areas of the phase plane. The signal representation and filtering operations are demonstrated using scattering responses from spheres and thin wires, and the prominent scattering features are identified and extracted.**

***Index Terms*—Scattering, time–frequency analysis.**

I. Background

Electromagnetic signals are traditionally expressed in either the time domain or the frequency domain. However, with the development of quantum optics, a different formulation has been introduced to take into account the particle-like nature of quantized electromagnetic fields (e.g., photons) [1], [4]. The mathematical formalism is known as coherent-state analysis. The basic components of the analysis are the coherent states which are of the form

$$g^{(p,\,q)}(x) = \frac{1}{\pi^{1/4}} e^{ipx} e^{-ipq/2} e^{-(x-q)^2/2} \tag{1}$$

where, in quantum mechanical terms, these are the photons that are characterized by a momentum p and a position coordinate q. Any signal $f(x)$ can be represented in the phase plane as $F(p,\,q)$ [4], [5] through the projections given by the well-known transform

$$F(p,\,q) = \int_{-\infty}^{\infty} f(x)\overline{g^{(p,\,q)}(x)}\,dx \tag{2}$$

where the bar denotes the complex conjugate. The corresponding inverse transform [3], [4] is given by

$$f(x) = \int_{-\infty}^{\infty}\int_{-\infty}^{\infty} F(p,\,q) g^{(p,\,q)}(x)\,dp dq. \tag{3}$$

If one makes the identification of x with ct (i.e., $x \to ct$ where c is the velocity of light), then the above transform becomes the well-known windowed Fourier transform. In signal processing, the windowed transform provides a localized time–frequency picture of a signal $f(t)$. The momentum p corresponds to the angular frequency ω (i.e., $p \to \omega$), and the coordinate q corresponds to the center of the window transform τ (i.e., $q \to \tau$). In this paper, we elect to keep the physics-based identity of the analysis and blend it with the signal-processing applications to foster a broader picture of the physical phenomena involved.

An attractive compact form of the coherent-state transform given by (2) can be developed with the aid of the Bargmann transform. In the Bargmann transform, the phase space coordinates q and p are combined together to form a complex variable $z = q - ip$. Utilizing the Bargmann transform, the phase space representation $F(p,\,q)$ of a function $f(x)$ becomes a complex function $F(z)$, and all the powerful techniques of complex variable theory are available for the representation and analysis of the transforms.

The Bargmann transform has been introduced by a number of investigators [1], [4]–[7], and is defined as

$$FBf(z) = \frac{1}{\pi^{1/4}} e^{-z^2/4} \int_{-\infty}^{\infty} e^{zx - x^2/2} f(x)\,dx. \tag{4}$$

The Bargmann transform is an isometry from the space of square integrable functions $L^2(\mathbb{R})$ to the space $L^2(\mathbb{C},\, e^{-|z|^2/2}\,dz)$ which is known as the Fock space $\mathcal{F}$. The Fock space is defined as

$$\mathcal{F} = \left\{ F\colon F \text{ is an entire function on } \mathbb{C},\ \|F\|_{\mathcal{F}}^2 = \int_{-\infty}^{\infty} |F(z)|^2 e^{-|z|/2}\,dz < \infty \right\} \tag{5}$$

where $z = q - ip$, and q and p are the phase plane coordinates.

The Fock space is the space of entire analytic functions defined in the whole complex plane $\mathbb{C}$. Describing a dynamical system in terms of its space position coordinate q and momentum p is known as the phase space representation.

The Bargmann transform can also be written in a traditional form using the phase space variables p and q as

$$Bf(z) = \frac{1}{\pi^{1/4}} e^{(p^2+q^2)/4} e^{ipq/2} \int_{-\infty}^{\infty} e^{-ipx - (x-q)^2/2} f(x)\,dx. \tag{6}$$

The corresponding inverse Bargmann transform in this form [1], [4] is

$$\begin{aligned} f(x) &= B^{-1} e^{|z|^2/4} F(x) \\ &= \frac{e^{-x^2/2}}{\pi^{1/4}} \int_{-\infty}^{\infty}\int_{-\infty}^{\infty} e^{\overline{z}x} e^{-\overline{z}^2/4} F(z)[e^{-|z|^2/4}\,dz], \\ & \qquad dz = dpdq. \end{aligned} \tag{7}$$

II. Hermite-Function Expansions

The set of Hermite functions is the natural basis for the Bargmann transform. This represents an important analytical tool for the representation of the signals. The orthogonal Hermite functions $\varphi_n(x)$ are

$$\varphi_n(x) = \frac{e^{-\frac{x^2}{2}}}{\pi^{1/4}} \frac{H_n(x)}{\sqrt{2^n n!}} \text{ with the Bargmann transform}$$

$$\zeta_n(z) = \frac{z^n}{\sqrt{2^n n!}} \tag{8}$$

where $H_n(x)$ is the Hermite polynomial. It is important to note that the Bargmann transform of the Hermite function is a monomial. Accordingly, an arbitrary function $f(x)$ represented in a Hermite function basis is

$$f(x) = \sum \alpha_n \varphi_n(x) \quad \alpha_n = \int_{-\infty}^{\infty} f(x)\varphi_n(x)\,dx \tag{9}$$

with a phase space transform of the form

$$F(z) = \sum \alpha_n \zeta_n(z). \tag{10}$$

Manuscript received December 10, 1997; revised December 10, 1997.

H. N. Kritikos is with the Department of Electrical Engineering, University of Pennsylvania, Philadelphia, PA 19104 USA (e-mail: kritikos@ee.upenn.edu).

J. G. Teti, Jr. is with Lambda Science, Inc., Wayne, PA 19087 USA (e-mail: drteti@lamsci.com).

Publisher Item Identifier S 0018-9480(98)02028-6.

0018–9480/98$10.00 © 1998 IEEE